Analyst

RSC Publishing

PAPER

An AC electrokinetics facilitated biosensor cassette for rapid pathogen identification†

Cite this: *Analyst*, 2013, **138**, 3660

Mengxing Ouyang,[abc] Ruchika Mohan,[ab] Yi Lu,[d] Tingting Liu,[d] Kathleen E. Mach,[ab] Mandy L. Y. Sin,[ab] Mason McComb,[e] Janhvi Joshi,[e] Vincent Gau,[e] Pak Kin Wong*[d] and Joseph C. Liao*[ab]

Received 1st February 2013
Accepted 6th April 2013

DOI: 10.1039/c3an00259d

www.rsc.org/analyst

To develop a portable point-of-care system based on biosensors for common infectious diseases such as urinary tract infection, the sensing process needs to be implemented within an enclosed fluidic system. On chip sample preparation of clinical samples remains a significant obstacle to achieving robust sensor performance. Herein AC electrokinetics is applied in an electrochemical biosensor cassette to enhance molecular convection and hybridization efficiency through electrokinetics induced fluid motion and Joule heating induced temperature elevation. Using *E. coli* as an exemplary pathogen, we determined the optimal electrokinetic parameters for detecting bacterial 16S rRNA in the biosensor cassette based on the current output, signal-to-noise ratio, and limit of detection. In addition, a panel of six probe sets targeting common uropathogenic bacteria was demonstrated. The optimized parameters were also validated using patient-derived clinical urine samples. The effectiveness of electrokinetics for on chip sample preparation will facilitate the implementation of point-of-care diagnosis of urinary tract infection in the future.

Introduction

There is significant interest in applying biosensor technologies to point-of-care (POC) diagnosis of infectious diseases[1–5] in order to improve clinical decision making and expedite delivery of appropriate treatment.[6] In contrast to diagnostic platforms based in centralized laboratories, POC biosensor devices offer advantages of small sample volume, rapid diagnosis, and potentially lower cost. Urinary tract infection (UTI) is one of the most common bacterial infections worldwide with an almost 50% lifetime prevalence.[1] Diagnostic challenges of UTI include significant delay of conventional culture-based diagnosis, multitude of potential pathogens with different antimicrobial susceptibility profiles, and overlapping symptoms caused by non-bacterial urinary tract diseases. These diagnostic challenges make UTI an ideal target application for biosensor technology to achieve POC diagnosis of common bacterial infections.[1]

We have previously reported 1 hour diagnosis of UTI using an electrochemical biosensor with a straightforward protocol consisting of sample lysis, sandwich hybridization of bacterial 16S rRNA with oligonucleotide probes, followed by amperometric detection.[7–10] In this assay, bacterial 16S rRNA[15,16] serves as the target analyte and provides a well-characterized molecular fingerprint, while oligonucleotide probe pairs (capture and detector) provide specific pathogen recognition elements. Detector probes are tagged for detection with horseradish peroxidase (HRP) to mediate the electron transfer required for amperometric detection. An array of amperometric sensors functionalized with a panel of probes with different specificities is used to interrogate an unknown clinical urine sample. Validation studies using clinical urine samples with a 16-sensor array demonstrated a diagnostic sensitivity of 89% and specificity of 97%.[10]

Molecular diagnostics using biosensors rely on highly specific recognition events in order to detect their target analytes.[11] Efficient mixing is needed to optimize the overall signal-to-noise ratio (SNR) of the biosensor and reproducibility of the results. Signal outputs are frequently limited by diffusion.[12,13] AC electrokinetics is one of the most promising techniques to simplify sample preparation steps and improve sensor performance.[14]

Among different AC electrokinetic phenomena, two electrohydrodynamic effects, namely AC electroosmosis and AC electrothermal flow (ACEF), can induce fluid motion in microchannels. AC electroosmosis dominates fluid flow under

[a]*Department of Urology, Stanford University, Stanford, California 94305-5118, USA. E-mail: jliao@stanford.edu*

[b]*Veterans Affairs Palo Alto Health Care System, Palo Alto, California 94304, USA*

[c]*Department of Mechanical and Biomedical Engineering, City University of Hong Kong, Kowloon Tong, Hong Kong SAR*

[d]*Department of Aerospace and Mechanical Engineering, The University of Arizona, Tucson, Arizona 85721, USA. E-mail: pak@email.arizona.edu*

[e]*GeneFluidics, Inc., Irwindale, California, 91010, USA*

† Electronic supplementary information (ESI) available. See DOI: 10.1039/c3an00259d

frequencies lower than 100 kHz,[15] but is negligible in high conductivity environments due to compression of the electrical double layer. Thus, it is unsuitable for biological and clinical assays involving highly conductive physiological and biological fluids.[16] ACEF, however, is effective in generating fluid motion in conductive solutions.[17–20] With ACEF, inhomogeneous temperature fields generated by non-uniform AC electric fields affect the permittivity and conductivity in the fluid. These permittivity and conductivity gradients lead to Coulombic and dielectric body forces in the fluid. As established by Ramos *et al.*,[21] assuming that the temperature advection is sufficiently small compared to conduction, the temperature of the fluid under steady state conditions can be determined using the simplified energy equation:

$$k\nabla^2 T + \sigma E^2 = 0 \quad (1)$$

where T is the temperature, E refers to the magnitude of the applied electrical field, k and σ represent the thermal conductivity and the electrical conductivity of the fluid, respectively.

Gradients in permittivity and conductivity in the fluid result in variations in charge density and electric field. With the assumption that the perturbed electrical field and advection of electric charge are much smaller than the applied electrical field and conduction, respectively, the time-averaged electrical force per unit volume for a non-dispersive fluid is described as:[21]

$$\vec{f}_{\mathrm{E}} = -0.5\left[\left(\frac{\nabla\sigma}{\sigma} - \frac{\nabla\varepsilon}{\varepsilon}\right)\cdot \overline{E}_0 \frac{\varepsilon\overline{E}_0}{1+(\omega\tau)^2} + 0.5\,|E_0|^2\,\nabla\varepsilon\right] \quad (2)$$

where $\tau = \varepsilon/\sigma$ is the charge relaxation time of the fluid medium. The first term and the second term on the right hand side of the equation refer to Coulombic force and dielectric force, respectively. The former force dominates at lower frequencies while the latter one governs at higher frequencies.

Previously, we demonstrated that ACEF induced mixing and heating enhanced electrochemical detection of bacterial 16S rRNA for UTI diagnosis.[16] However, to this point our biosensor assays have been performed in an open system, with exposed sensors and washing steps performed by manually rinsing the sensor surface. In order to implement ACEF in a POC device for UTI diagnosis, the biosensor array needs to be incorporated into an enclosed fluidic system. However, little is known about the effects of the channel, which represents significantly different thermal and fluidic boundary conditions, on ACEF for enhancing the sensor performance. Furthermore, the challenges of biosensing in an enclosed fluidic system including maintenance of low background signal and robust operation with clinical urine samples should be addressed. In the present work, we enclosed the biosensor in a cassette and optimized the ACEF conditions for nucleic acid-based hybridization of uropathogens. Using the biosensor cassette we determined the specificity and sensitivity of a panel of six probe pairs targeting common bacterial uropathogens. Finally, clinical samples were tested using the optimized parameters in the biosensor cassette to verify the applicability of the system for point-of-care diagnosis of UTI.

Material and methods

Probe design

Table S1† lists the panel of previously validated capture and detector oligonucleotide probe pairs targeting bacterial 16S rRNA.[10,22] The universal (UNI) probe pair detects all pathogens and the EB probe pair targets the *Enterobacteriaceae* family, which constitute the majority of enteric-derived gram-negative uropathogens. The species-specific probes include EC, PM, PA, and EF targeting *E. coli*, *P. mirabilis*, *P. aeruginosa*, and *E. faecalis*, respectively. As a positive control, a randomly generated synthetic target (5′-GATGTTTGTGCGACTTATTTTTGGAGTTTTTTATTGT AGGTAGT-3′) was used with positive control capture and detector probes. For a negative control, a randomly generated sequence with no known homology was used as the capture probe in conjunction with a non-complementary detector probe.

Electrochemical biosensor cassette

The biosensor cassette is composed of an array of 16 biosensors covered with a plastic manifold to create the enclosed fluidic chamber. The 16-biosensor arrays were fabricated on a 2.5 cm by 7.5 cm plastic substrate by depositing Au electrodes using photolithography techniques (GeneFluidics, Irwindale, CA). Each sensor was composed of a planar configuration of working, auxiliary, and reference electrodes. The gap distance between the working electrode and the auxiliary electrode was 1.2 mm. As previously described, sensor arrays were functionalized by incubating 6 μL of 0.05 μM thiolated capture probe and 300 μM 1,6-hexanedithiol (HDT) in TE buffer on the working electrode of each sensor at 4 °C overnight. To complete functionalization, 6 μL of 1 mM 6-mercapto-1-hexanol (MCH) solution was spotted on the working electrodes and incubated for 50 min at room temperature.[22] After sensor functionalization with the capture probes, a laser machined 16-well plastic manifold was bonded to the sensor surface with the electrode area exposed, then a cover was fixed on the top to form an enclosed chamber with two small holes of diameter 2 mm to serve as the inlet and outlet ports (Fig. 1). The biosensor cassette simulates the cartridge that will be used in the final POC device.

ACEF facilitated detection of bacterial 16S rRNA

Cultured bacteria in LB medium at the desired concentration or clinical urine samples were lysed and the detector probe solution was added as previously described.[10] 30 μL of the hybridized lysate was delivered onto each sensor by pipetting the solution through the inlet port of the manifold to cover the electrodes.

For diffusion-based hybridization, the lysate was pre-incubated for 10 min at 37 °C in solution, then applied to the sensor and incubated for additional 15 minutes at 37 °C. For ACEF facilitated hybridization, the lysate was directly applied to the sensor. To generate AC electrothermal flow in the sensor chamber, a square wave AC potential was applied across the working and auxiliary electrodes using a function generator (HP, 33210A) and monitored using a digital oscilloscope. After hybridization, the sensor was washed with 1× SSC buffer *via* the

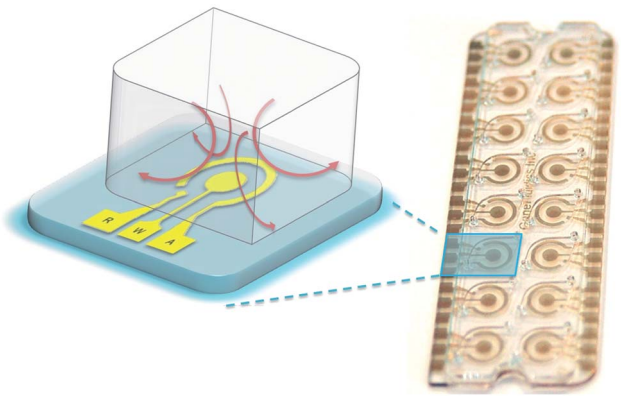

Fig. 1 Photo of the biosensor cassette containing an array of 16 electrochemical biosensors (right). The schematic (left) shows an enclosed biosensor during AC electrothermal flow (ACEF)-facilitated hybridization. The red flows represent bulk fluid motion generated by Joule heating. Each electrochemical biosensor consisted of three planar electrodes: working (W), reference (R), and auxiliary (A). ACEF is applied between the working and the auxiliary electrode.

inlet and outlet ports. Then, 30 μL of 0.5 U ml^{-1} anti-FITC POD (Roche) in PBS and 0.5% casein were added to the chamber and incubated at room temperature for 15 min. After washing the sensor array with 1× SSC buffer three times, 30 μL of the HRP substrate H_2O_2 and the electron transfer mediator TMB (K-Blue low activity solution, Neogen, 330176) was added to each well using a multi-channel pipette for immediate amperometric reading. The current of each sensor was measured simultaneously using a multichannel potentiostat (GeneFluidics) at a fixed voltage of −200 mV with respect to the reference electrode. The electro-reduction current was measured at 60 s after the redox reaction reached quasi-steady-state. The cutoff threshold for detection was defined as three times the standard deviation above the negative control (NC) for all 6 species of probe pairs, *i.e.* NC + 3SD (log_{10} unit).[10]

Clinical urine samples

Patient urine samples were collected with approval from Stanford University Institutional Review Board (IRB) and Veterans Affairs Palo Alto Health Care System (VAPAHCS) Research and Development committee. Urine samples were collected and stored at −80 °C until analysis.

Infrared thermometry

Heat generation in the biosensor cassette with ACEF was measured using a mid-wavelength infrared camera (SC6700; FLIR, Wilsonville, OR). The mid-wavelength infrared camera system detects the wavelength from 3 μm to 5 μm. In the experiment, the camera is placed 10 cm above the biosensor cassette loaded with the same hybridization buffer with appropriate AC potential at 200 kHz as in the electrochemical sensing experiment. A video was taken using a frame rate of 1 fps to capture the dynamics of the temperature. Finally, a thermal stack image file was exported to extract the temperature information using the software FLIR ExaminIR and the temperature on the working electrode is reported.

Velocity measurement

To visualize the fluid motion in the biosensor cassette, 200 nm polystyrene fluorescent particles (F8810; Invitrogen, Carlsbad, CA) were added to the hybridization buffer. AC potential was applied to the biosensor cassette in the hybridization step. The movement of the particles was traced and recorded using an inversed epi-fluorescent microscope (DMI 4000B; Leica, Frankfurt, Germany) with a digital charge-coupled device (CCD) camera (DMK31AF03; Image Source, Bremen, Germany). The particle velocity was estimated by particle tracking based on the recorded trajectories and time span.

Results

Infrared thermometry of the hybridization reaction

Temperature is a critical parameter for hybridization of capture and detector probes to the target bacterial 16S rRNA and to maintain the analytical sensitivity and specificity of the electrochemical sensor assay. In ACEF facilitated hybridization, heat generation is regulated by the applied voltage and conductivity of the buffer. The temperature in the system can also be affected by the chamber design, which modulates the thermal boundary conditions. To determine ACEF parameters that will result in optimal hybridization conditions, we measured the temperature of the lysate within the biosensor cassette using infrared thermometry.

Fig. 2 shows the lysate temperature above the working electrode and gap area at voltage of 6 Vpp, 7 Vpp, 8 Vpp and 9 Vpp all at a frequency of 200 kHz. Each measurement was carried out for 15 minutes. The heating time constant is approximately 1.5 min under our experimental conditions. The temperature increases with the applied voltage with a power exponent of 2.11. The exponent is in good agreement with the theoretically predicted exponent of 2 (*i.e.*, $\Delta T \sim V^2$).[21] At, 6 Vpp, 7 Vpp, 8 Vpp and 9 Vpp, the steady state temperatures on the working electrodes were 42.6 ± 0.3 °C, 48.5 ± 0.4 °C, 58.5 ± 0.4 °C and 68.6 ± 0.8 °C, respectively. With proper control of the applied voltage

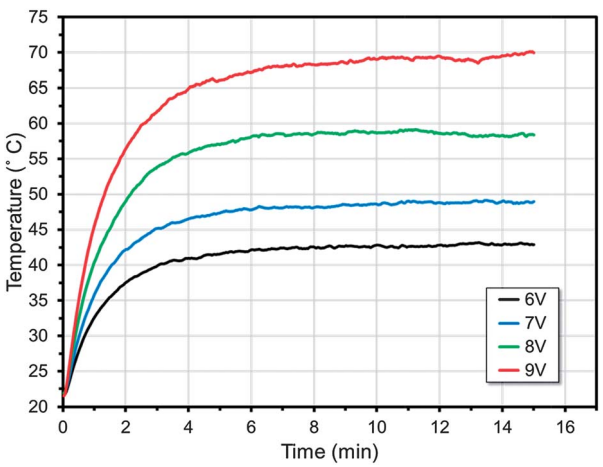

Fig. 2 Temperature measurement above the working electrode during ACEF as measured by infrared thermometry. Voltages of 6 Vpp, 7 Vpp, 8 Vpp and 9 Vpp were used.

temperature, the sensor temperature can be controlled to values comparable to the calculated melting temperature of the EC probes, which ranges from 52.5 °C to 59.9 °C.

Quantification of ACEF facilitated mixing

Fluorescence particles were used to quantify ACEF in the biosensor cassette by particle tracking. We measured the particle velocity at different applied voltages (7 Vpp to 9 Vpp). In general, higher particle velocity was observed at higher voltage. However, bubble generation was observed at 9 Vpp due to electrolysis. At 7 Vpp and 8 Vpp, the maximum velocities were 68.3 μm s^{-1} and 118.9 μm s^{-1}, respectively. Based on these observations, we conclude that ACEF at 8 Vpp provides the fastest fluid advection in the sensor chamber for sensor enhancement without inducing bubbles.

Hybridization duration

To determine the optimal duration of ACEF for the hybridization reaction, we compared biosensor cassette performance using diffusion *versus* ACEF facilitated hybridization from 2.5 min to 15 min. For diffusion-based hybridization, the lysate was pre-incubated off-chip with the detector probe for 10 min at 37 °C followed by 15 minutes on chip hybridization at 37 °C. For ACEF facilitated hybridization, off-chip pre-hybridization with the detector probe was not used. *E. coli* was serially diluted and tested from concentrations ranging from 8×10^1 cfu ml^{-1} to 8×10^6 cfu ml^{-1} for both conditions. Similar SNRs were achieved with ACEF facilitated hybridization for 5 min and diffusion-based hybridization for 15 min. Since the 10 min off-chip pre-hybridization is not required in ACEF facilitated hybridization, ACEF presents a 20 min reduction in the assay time and a significant simplification of the assay protocol. Given the same duration of on chip hybridization (15 min) the SNR of biosensor detection of *E. coli* was improved by ~1.5 fold by ACEF. Moreover, we observed improvement of SNR in accordance with the increase of ACEF facilitated hybridization time from 2.5 min to 15 min. When the hybridization duration was increased to 20 min or higher, bubble formation was observed and the SNR of the biosensor cassette dropped significantly (data not shown), suggesting possible degradation of the electrodes.

Voltage for ACEF facilitated hybridization

Electrochemical sensor assays at different ACEF voltages were conducted to compare the overall signal output. As shown in Fig. 3, the overall SNR improved as the voltage was increased from 6 to 8 Vpp. Consistent with the fluid velocity measurement, the fluid advection was maximized at 8 Vpp without bubble generation. The optimal voltage value at 8 Vpp also agreed with the temperature measurement, which was below the melting temperature. As shown in Fig. 3 inset, there was a decreasing trend of the background signal with increasing voltage up to 8 Vpp. At 9 Vpp, the SNR, however, dropped significantly. The reduction in SNR can be understood by a combination of signal reduction and background increase. The signal reduction is likely due to the temperature exceeding the melting temperature of the probes. The increase in background could be a result of bubble generation and damage to the sensor. Taken together, our data suggest that ACEF at 8 Vpp at 200 kHz is optimal for hybridization in the biosensor cassette.

Limit of detection

Under the optimized ACEF condition in the biosensor cassette, the LOD for the EC probe pairs targeting *E. coli*, the most common uropathogen, was determined to be 3.78×10^3 cfu

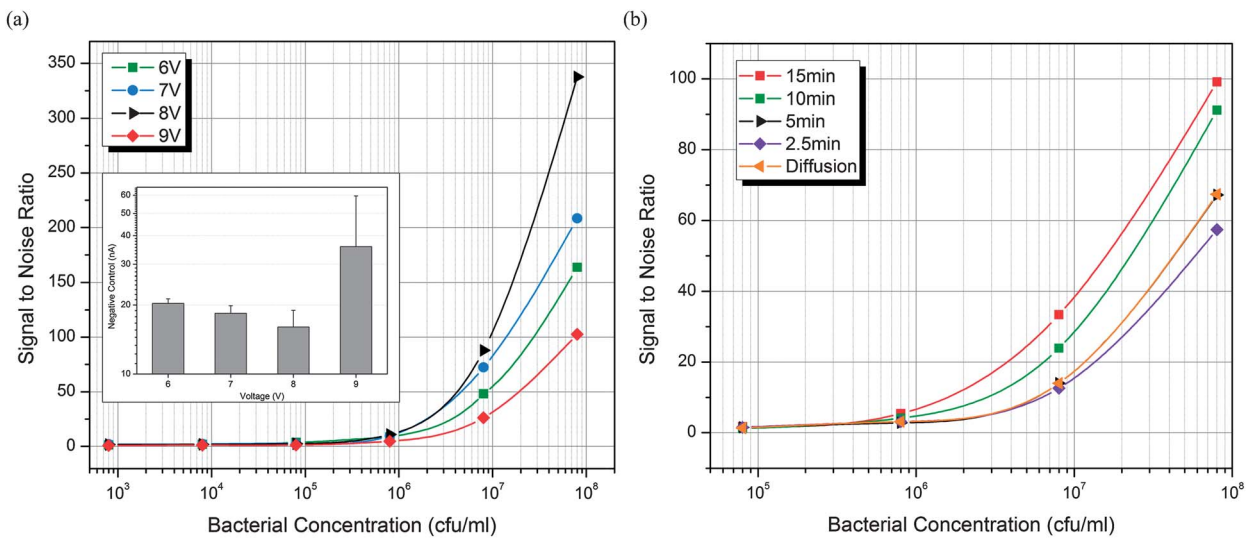

Fig. 3 Optimizing ACEF parameters to improve electrochemical detection of 16S rRNA of bacterial pathogens. (a) ACEF voltage dependency of an enclosed biosensor array. SNR of the biosensor under different *E. coli* clinical isolate concentrations is plotted. ACEF voltage from 6 Vpp to 9 Vpp was used. Inset figure: negative control signal output with different applied voltages is plotted on a log scale on the *Y* axis. Error bars represent the standard deviation from duplicate experiments. (b) Biosensor array output comparison using different ACEF durations at 7 Vpp applied voltage.

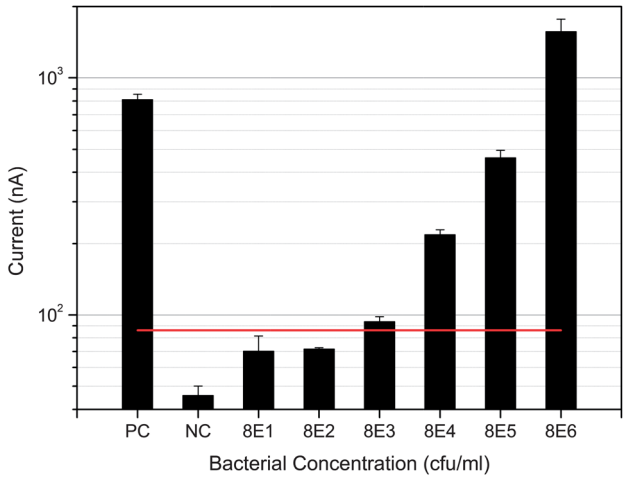

Fig. 4 Limit of detection of pathogen detection using optimized ACEF parameters. Output current (nA) of pathogenic *E. coli* concentrations from 8×10^1 cfu ml^{-1} to 8×10^6 cfu ml^{-1}, along with the positive control (PC) and the negative control (NC), using synthetic targets is plotted on a log scale on the *Y* axis. Error bars represent the standard deviation of duplicate experiments. The red line over the bars represents the threshold, defined as the negative control plus 3SD ($\log_{10}$ unit).

ml^{-1} (Fig. 4). Using the same ACEF-facilitated hybridization conditions, we evaluated the LOD for 5 additional probe pairs. Significant improvement for all 6 probe pairs was observed with our ACEF conditions compared to diffusion based hybridization. Among them, *E. coli* detection exhibited the most significant enhancement of ~10 fold, followed by ~9 fold enhancement for detection of *P. aeruginosa* with the PA probes. The 4 other probes showed ~2 fold improvement in LOD. The results demonstrate the general applicability of ACEF-facilitated hybridization for pathogen detection.

Probe specificity

To evaluate the analytical specificity of bacterial detection using the biosensor cassette with the EC probe optimized ACEF parameters, we tested 14 commonly encountered bacterial uropathogens against a panel of 6 probes. A sensor output greater than 3 standard deviation above background was deemed as a positive signal. Sensor outputs for assays with each of the 6 probe pairs tested are shown in Fig. 5 and compiled in ESI Table 1.† *E. coli*, *E. faecalis*, *P. aeruginosa* and *P. mirabilis* were detected specifically with EC, EF, PA, and PM probes, respectively, while the EB probe detected all species from the *Enterobacteriaceae* family. Additionally, the UNI probe was positive for all the bacterial species tested. Despite the higher background signal in the biosensor cassette with high bacterial concentration (as compared to the no bacteria control in the LOD measurements), the specificity of the probes was maintained using the same definition of the threshold previously chosen for an open system.

Validation using clinical urine samples

We tested seven clinical urine samples using the biosensor cassette with the optimized ACEF parameters. Each urine sample was tested on a 16-sensor array functionalized with duplicates of the 6 probe pairs targeting 16S rRNA, and positive and negative controls. Fig. 6 shows the data from representative urine samples with three different pathogen profiles. Sample 1 contained a single species targeted by a species-specific probe on the array, sample 2 contained an *Enterobacteriaceae* species not targeted by a species-specific probe on the array, and sample 3 contained multiple species targeted by species-specific probes on the array. The positive signal profile of the ACEF enhanced, biosensor cassette assays for the three samples shown in Fig. 6,

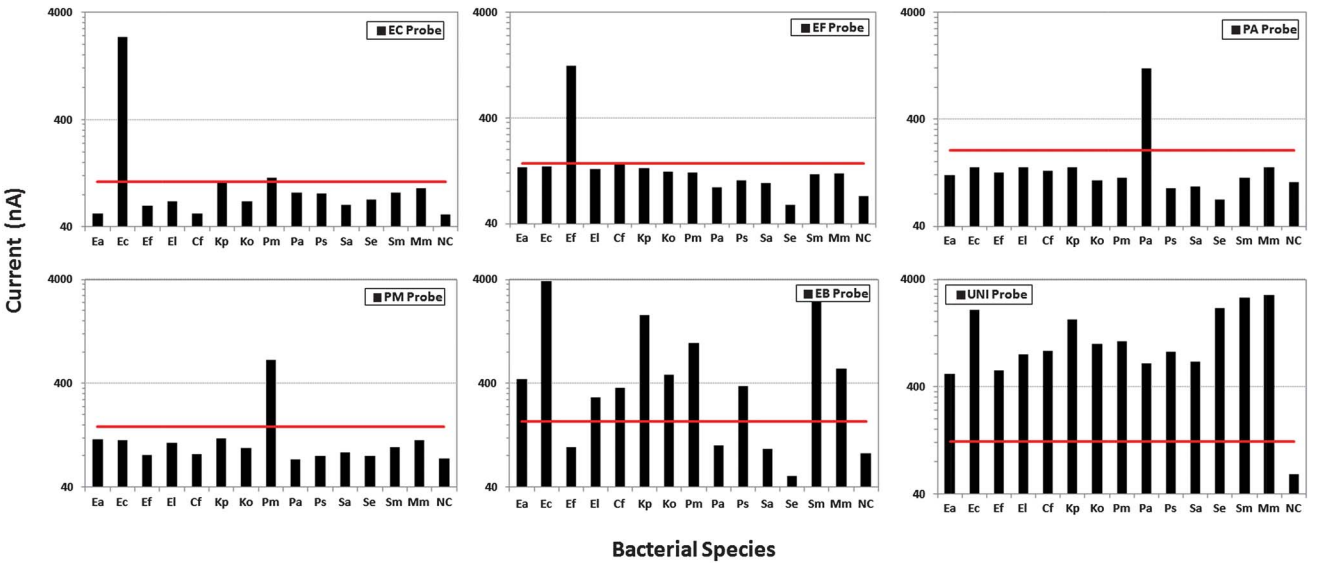

Fig. 5 Specificity experiments of 6 probe pairs. EC, PM, PA and EF probe pairs targeting *E. coli*, *P. mirabilis*, *P. aeruginosa*, and *E. faecalis*, respectively. EB probe pair targeted *Enterobacteriaceae* family (*e.g. E. coli* and *P. mirabilis*). The universal (UNI) probe pair targeted all bacterial species tested. For negative control (NC), synthetic oligonucleotide targets are used with non-complimentary probe pairs. The red lines over the bars represent the threshold for all 6 probe pairs, defined as the negative control of each probe pair plus 3SD ($\log_{10}$ unit).

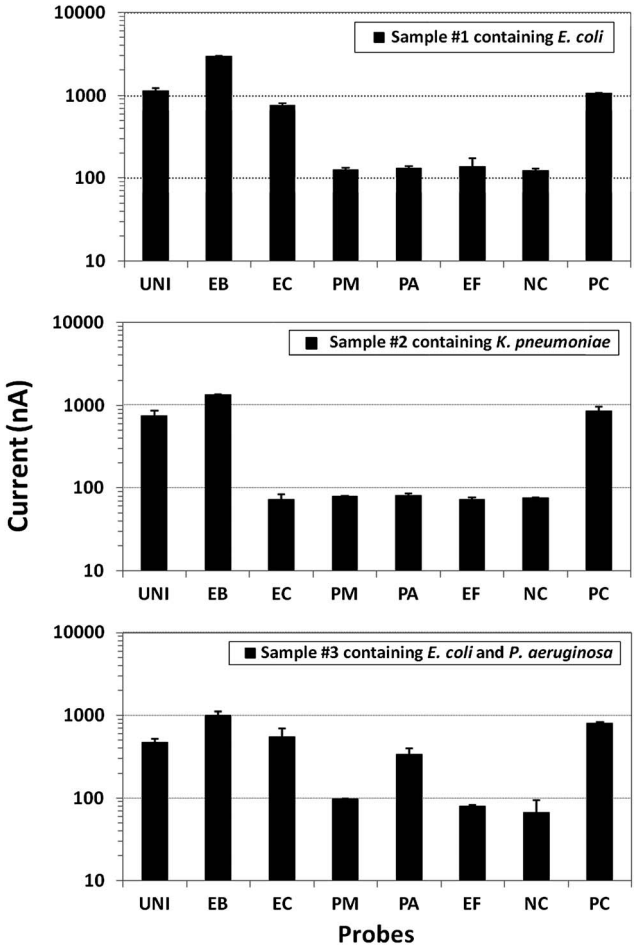

Fig. 6 Direct electrochemical detection of bacterial pathogens from clinical samples using optimized ACEF parameters. *X*-axis shows the 6 bacterial probe pairs, negative (NC) and positive controls (PC). Current output of the biosensor cassette is plotted on the *Y* axis. The biosensor cassette results are compared with urine culture results from a clinical microbiology laboratory. Sample #1 contained *E. coli* (1.0×10^8 cfu ml^{-1}), which is targeted by the UNI, EB and EC probe; sample #2 contained *K. pneumoniae* (7.3×10^8 cfu ml^{-1}), which is targeted by UNI and EB probes; and sample #3 contained both *E. coli* (1.5×10^7 cfu ml^{-1}) and *P. aeruginosa* (5×10^7 cfu ml^{-1}), which is targeted by UNI, EB, EC and PA probes. Error bars represent the standard deviation of duplicate sensor results.

as well as the other samples tested, was consistent with the clinical microbiology laboratory report.

Discussion

In this paper we report the initial steps of translating an in-laboratory open biosensor array into a biosensor cassette for eventual POC application in UTI diagnostics. Our previously characterized electrochemical biosensor was enclosed in a manifold with inlet and outlet ports for fluid delivery. Fluid volume and chamber dimensions can influence ACEF, therefore we studied the optimal ACEF parameters for the enclosed fluidic system. ACEF was adjusted to generate the appropriate temperature and mixing for nucleic acid hybridization based detection of pathogens in the chamber. Using ACEF for temperature regulation simplified the assay by obviating the need for off chip sample hybridization and use of an incubator. Additionally, compared with diffusion, the ACEF optimized parameters were able to reduce hybridization time while maintaining probe specificity and improving assay sensitivity. In addition, we used the ACEF optimized biosensor cassette to test clinical urine samples for the presence of pathogen. In all samples tested, the interpretation of biosensor results was consistent with the clinical microbiology laboratory report, validating the possibility of using enclosed biosensor arrays for rapid UTI diagnosis.

Hybridization efficiency

In the biosensor cassette assay chamber mixing is dominated by diffusion.[6] As diffusion is inefficient, application of ACEF not only serves to heat the solution to the appropriate hybridization temperature but also induces fluid advection in the enclosed fluidic system to increase the capturing efficiency between probes and target and reduce non-specific binding.

For the optimization of ACEF parameters, several factors including current output, background signal, SNR, and LOD were evaluated. Among them, LOD, which represents the lowest detectable analyte concentration, was considered the most important. The EC probe was used here for ACEF optimization, as *E. coli* is the most common uropathogen. Consistent with the approach, the EC probe showed the greatest improvement in LOD. The optimal ACEF parameters for other probe sequences may differ due to the difference in melting temperature and binding efficiency. However, the LOD for the 6 different probe pairs tested here all improved to the level below the standard clinical cutoff for UTI (1×10^5 cfu ml^{-1}).

POC device development

Current efforts are being devoted to further integration of the biosensor cassette into a fully automated microfluidic cartridge and to development of electrokinetic compatible components for portable devices. Since electrochemical sensing electrodes are involved, electrokinetics provides an effective system integration strategy. Electrokinetics has the potential to serve as a multi-functional component in a POC device and can be applied to both sample preparation and sensor enhancement simply by adjusting the parameters.[23] Electrokinetics could also be used to concentrate bacteria to improve sensitivity, separate unwanted components, and serves as a mixing mechanism for automated sample preparation.[16,17,24] Another inherent advantage of electrokinetics is the cost-effectiveness and simplicity of the electronic interface for implementing various fluidic operations, which are key requirements in point-of-care diagnostics.[14]

Conclusions

In conclusion, we have demonstrated rapid bacterial detection using a biosensor cassette with probes targeting 16S rRNA. This represents an important intermediate step towards our long term goal of translating molecular diagnosis of UTI from laboratory to POC settings. By incorporating ACEF into the hybridization step of the biosensor cassette, we improved our overall SNR and hybridization efficiency, as well as reduced the

incubation time. We determined that 8 Vpp and 200 kHz were the optimal ACEF parameters in our experimental setup. The overall LOD for detection of uropathogens was 10^3 to 10^4 cfu ml^{-1}, which is one to two orders of magnitude below the clinical cutoff for UTI diagnosis. Direct testing of clinical urine samples was consistent with clinical microbiology laboratory reports, highlighting the potential of our enclosed biosensor array for rapid UTI diagnostics.

Acknowledgements

Supported by National Institutes of Health U01 AI082457 and National Science Foundation Collaborative Research Grant 0901440 (J.C.L.), and NIH DP2 OD007161 (P.K.W.) and NIH R44 AI 088756 (V.G.). Mengxing Ouyang acknowledges the financial support from Global Scholarship Programme for Research Excellence – CNOOC Grants (2011–2012) from the Chinese University of Hong Kong as a visiting student researcher to Stanford University.

Notes and references

1 K. E. Mach, P. K. Wong and J. C. Liao, *Trends Pharmacol. Sci.*, 2011, **32**, 330–336.
2 J. M. Song and H. T. Kwon, *Methods Mol. Biol.*, 2009, **503**, 325–335.
3 M. Tichoniuk, D. Gwiazdowska, M. Ligaj and M. Filipiak, *Biosens. Bioelectron.*, 2010, **26**, 1618–1623.
4 N. V. Zaytseva, V. N. Goral, R. A. Montagna and A. J. Baeumner, *Lab Chip*, 2005, **5**, 805–811.
5 A. Niemz, T. M. Ferguson and D. S. Boyle, *Trends Biotechnol.*, 2011, **29**, 240–250.
6 V. Gubala, L. F. Harris, A. J. Ricco, M. X. Tan and D. E. Williams, *Anal. Chem.*, 2012, **84**, 487–515.
7 J. C. Liao, M. Mastali, V. Gau, M. A. Suchard, A. K. Moller, D. A. Bruckner, J. T. Babbitt, Y. Li, J. Gornbein, E. M. Landaw, E. R. McCabe, B. M. Churchill and D. A. Haake, *J. Clin. Microbiol.*, 2006, **44**, 561–570.
8 J. C. Liao, M. Mastali, Y. Li, V. Gau, M. A. Suchard, J. Babbitt, J. Gornbein, E. M. Landaw, E. R. McCabe, B. M. Churchill and D. A. Haake, *J. Mol. Diagn.*, 2007, **9**, 158–168.
9 K. E. Mach, C. B. Du, H. Phull, D. A. Haake, M. C. Shih, E. J. Baron and J. C. Liao, *J. Urol.*, 2009, **182**, 2735–2741.
10 R. Mohan, K. E. Mach, M. Bercovici, Y. Pan, L. Dhulipala, P. K. Wong and J. C. Liao, *PLoS One*, 2011, **6**, e26846.
11 T. G. Drummond, M. G. Hill and J. K. Barton, *Nat. Biotechnol.*, 2003, **21**, 1192–1199.
12 T. M. Squires, R. J. Messinger and S. R. Manalis, *Nat. Biotechnol.*, 2008, **26**, 417–426.
13 H. C. Feldman, M. Sigurdson and C. D. Meinhart, *Lab Chip*, 2007, **7**, 1553–1559.
14 M. L. Sin, J. Gao, J. C. Liao and P. K. Wong, *J. Biol. Eng.*, 2011, **5**, 6.
15 H. Morgan and N. G. Green, *AC electrokinetics: colloids and nanoparticles*, Research Studies Press LTD., Hertfordshire, England, 2003.
16 M. L. Sin, T. Liu, J. D. Pyne, V. Gau, J. C. Liao and P. K. Wong, *Anal. Chem.*, 2012, **84**, 2702–2707.
17 J. Gao, M. L. Sin, T. Liu, V. Gau, J. C. Liao and P. K. Wong, *Lab Chip*, 2011, **11**, 1770–1775.
18 M. Sigurdson, D. Wang and C. D. Meinhart, *Lab Chip*, 2005, **5**, 1366–1373.
19 C. Meinhart, D. Wang and K. Turner, *Biomed. Microdevices*, 2003, **5**, 139–145.
20 F. Bottausci, C. Cardonne, C. Meinhart and I. Mezic, *Lab Chip*, 2007, **7**, 396–398.
21 A. Ramos, H. Morgan, N. G. Green and A. Castellanos, *J. Phys. D: Appl. Phys.*, 1998, **31**, 2338–2353.
22 S. Campuzano, F. Kuralay, M. J. Lobo-Castanon, M. Bartosik, K. Vyavahare, E. Palecek, D. A. Haake and J. Wang, *Biosens. Bioelectron.*, 2011, **26**, 3577–3583.
23 M. L. Y. Sin, V. Gau, J. C. Liao and P. K. Wong, *JALA*, 2010, **15**, 426–432.
24 J. Gao, R. Riahi, M. L. Sin, S. Zhang and P. K. Wong, *Analyst*, 2012, **137**, 5215–5221.

